



Preparation of astaxanthin-loaded DNA/chitosan nanoparticles for improved cellular uptake and antioxidation capability



Qian Wang^{b,1}, Yingyuan Zhao^{a,1}, Lei Guan^a, Yaping Zhang^a, Qifeng Dang^b, Ping Dong^a, Jing Li^{a,*}, Xingguo Liang^{a,*}

^a College of Food Science and Engineering, Ocean University of China, Qingdao 266003, PR China

^b College of Marine Life Science, Ocean University of China, Qingdao 266003, PR China

ARTICLE INFO

Article history:

Received 30 August 2016

Received in revised form 7 December 2016

Accepted 16 January 2017

Available online 17 January 2017

Keywords:

Nanodispersion

Nanoparticle

Astaxanthin

Chitosan

DNA

Cellular uptake

Antioxidant

ABSTRACT

DNA/chitosan co-assemblies were initially used as nanocarriers for efficient astaxanthin encapsulation and delivery. The obtained astaxanthin-loaded DNA/chitosan (ADC) colloidal system was transparent and homogenous, with astaxanthin content up to 65 µg/ml. Compared to free astaxanthin, ADC nanoparticles with an astaxanthin concentration as low as 3.35 nM still showed a more powerful cytoprotective effect on H₂O₂-induced oxidative cell damage, and improved cell viability from 49.9% to 61.9%. The ROS scavenging efficiency of ADC nanoparticles was as high as 54.3%, which was 2-fold higher than that of free astaxanthin. Besides this, ADC nanoparticles were easily engulfed by Caco-2 cells in a short time, indicating that the encapsulated astaxanthin could be absorbed through endocytosis by intestinal epithelial cells. The improved antioxidation capability and facilitated cellular uptake enabled the ADC nanoparticles to be good candidates for efficient delivery and absorption of astaxanthin.

© 2017 Elsevier Ltd. All rights reserved.

1. Introduction

Astaxanthin is a carotenoid that has a stronger antioxidant activity than vitamin E and beta-carotene (Naguib, 2000) due to its conjugated double bond and hydroxyl group. However, the low stability and solubility of astaxanthin (Kittikaiwan, Powthongsook, Pavasant, & Shotipruk, 2007; Park, Ahn, Choi, Lee, & Lee, 2014) results in poor bioavailability and antioxidant capacity, which significantly restricts its application in fields such as medicine, cosmetics and functional food.

To improve the solubility, stability and bioavailability of astaxanthin, several strategies have been investigated, including micro-encapsulation (Bustos-Garza, Yáñez-Fernández, & Barragán-Huerta, 2013), incorporation into liposomes (Peng, Chang, Peng, & Chyau, 2010) and nanoemulsion (Majeed, 2011). Higuera-Ciapara and his coworkers utilized a chitosan matrix cross-linked with glutaraldehyde for microencapsulation of astaxanthin to enhance the stability of astaxanthin (Higuera-Ciapara, Felix-Valenzuela,

Goycoolea, & Argüelles-Monal, 2004). However, the addition of chemical crosslinking agents was not safe for daily intake, and the micro-sized particles neither dispersed well in water nor enhanced the cellular uptake efficiency (Kulkarni & Feng, 2013). To obtain water-dispersible astaxanthin, Anarjan, Tan, Nehdi, and Ling (2012) prepared astaxanthin colloidal particles showing higher cellular uptake than pure astaxanthin. As mention above, a few of the absorption mechanisms of astaxanthin colloidal system have been revealed, while, in reference to the antioxidant activity of astaxanthin-loaded nanoparticles *in vitro*, little has been investigated.

Chitosan has been widely used as a drug carrier thanks to its nontoxicity, antibacterial activity and biocompatibility (Thanou, Verhoef, & Junginger, 2001). Chitosan is also proved to be a potential penetration enhancer to promote drug absorption (Behrens, Pena, Alonso, & Kissel, 2002; Mohammadi et al., 2011; Yamamoto, Kuno, Sugimoto, Takeuchi, & Kawashima, 2005). Tachaprutinun et al. prepared an astaxanthin nanosystem by encapsulating astaxanthin into a chitosan derivative (Tachaprutinun, Udomsup, Luadthong, & Wanichwecharungruang, 2009), but there was no further study on either absorption mechanisms or antioxidant activity of the above astaxanthin nanosystem. On the basis that chitosan can interact with negatively charged macromolecules and assemble into nanoparticles by non-covalent

* Corresponding authors.

E-mail addresses: wangqian366616552@163.com (Q. Wang), anxiaoying2010@163.com (Y. Zhao), 2547141392@qq.com (L. Guan), 626517093@qq.com (Y. Zhang), qfdang@ouc.edu.cn (Q. Dang), dongping@ouc.edu.cn (P. Dong), lijou@ouc.edu.cn (J. Li), liangxg@ouc.edu.cn (X. Liang).

¹ These authors contributed equally to this work.

interaction (Cui & Mumper, 2001), such as chitosan/sodium alginate nanoparticles (Li et al., 2015) and chitosan/poly- γ -glutamic acid nanoparticles (Sonaje et al., 2009). Many studies have focused on chitosan nanocarriers to encapsulate short gene sequences with low molecular weight (≤ 8 Kb), including siRNA and plasmid DNA (Layek & Singh, 2017). The application of chitosan as promising gene delivery vectors supported our speculation that linear long-chain natural DNA (≥ 20 Kb) could also induce the aggregation of chitosan and form nano-sized co-assemblies. As is widely known, natural nucleic acids are inherently biocompatible and have low or no immunogenic properties, making them ideal materials for both *in vitro* and *in vivo* applications. Actually, humans eat up to 2 g of nucleic acids each day. A non-covalent co-assembly of DNA with chitosan can not only control the rate of DNA hydrolysis (Hansen, 2002; Yan et al., 2013; Yue et al., 2011), but also maintain the molecular structure and properties of double helix DNA. For example, the stacked bases along the helix axis enable the DNA skeleton to bind small molecules via intercalation, groove binding and electrostatic interaction, which renders DNA an efficient drug-loading biomaterial.

In this study, chitosan and salmon sperm DNA as oppositely-charged biomaterials were used to fabricate a water dispersible nanocarrier system for astaxanthin loading and delivering. To understand the absorption effect of astaxanthin-loaded DNA/CS (ADC) nanoparticles as potential antioxidants, the cellular uptake and antioxidant capability of ADC nanoparticles were primarily investigated *in vitro*.

2. Materials and methods

2.1. Materials

Astaxanthin, fluorescein isothiocyanate (FITC), dichloro-fluorescein diacetate (DCFH-DA) and salmon sperm DNA were obtained from Sigma (St. Louis, USA). Chitosan (80 KDa, 91% deacetylation) was obtained from the Australia Hing Biological Technology Co, LTD (Zhejiang, China). 3-(4,5-Dimethylthiazol-2-yl)-2, 5-diphenyl-tetrazolium bromide (MTT) and Amresco were obtained from Gibco. All the other reagents and solvents were of analytical grade.

Caco-2 and L929 cells were obtained from the American Type Culture Collection (Rockville, MD, USA). Cells were cultured in Dulbecco's modified eagle medium (DMEM) (Gibco, Grand Island, NY, USA) containing 10% fetal calf serum and incubated in a humidified atmosphere containing 5% CO₂ at 37 °C.

2.2. Preparation of astaxanthin-loaded DNA/chitosan (ADC) nanoparticles

Astaxanthin was firstly dissolved in a specified volume of ethanol to get a saturated astaxanthin-ethanol solution, and then the mixture was centrifuged at 8000g for 5 min to obtain a clear supernatant for subsequent experimental use. Briefly, 60 ml of astaxanthin-ethanol solution was premixed with 80 ml of chitosan solution (0.02 mg/ml, pH 6) under magnetic stirring for 3 min. Then, 40 ml of salmon sperm DNA solution (0.02 mg/ml) was added. The mixture was then vacuum-evaporated with a rotary evaporator (Buchi RE 121, Switzerland) at 32 °C for 30 min to remove ethanol. Finally, the ADC nanodispersion was obtained and stored at 20 °C under light and argon protection for further use.

For comparison, empty nanocarriers, DNA/chitosan (DNA/CS) nanoparticles were prepared by mixing 80 ml of chitosan solution (0.02 mg/ml, pH 6) with 40 ml of salmon sperm DNA solution (0.02 mg/ml) under magnetic stirring (500 rpm) for 30 min.

2.3. Characterization of the ADC nanoparticles

The particle size, polydispersity index (Pdl) and zeta potential of the prepared nanoparticles were measured with a Zetasizer (3000HS, Malvern Instruments, Worcestershire, UK). Each sample (1 ml) was added into the cell. In the card slot, the test angle was 90°, the test temperature was 25 °C, the equilibrium time was 120 s, and the cycle times was 90 times.

The morphology of the ADC nanoparticles was studied using Field Emission Scanning Electron Microscopy (FESEM, JSM-6700F, Japan) (Zhao et al., 2010) and Transmission Electron Microscopy (TEM, JEM-2010, Japan) (Yang, Gao, Bao, Su, & Chen, 2013), respectively.

The astaxanthin content in prepared ADC nanodispersion was measured by using a P230II type of HPLC system (Elite, Dalian, China), equipped with a YLT C18 column (4.6 × 200 mm, 5 μ m) and an isocratic mobile phase consisting of 85% methanol, 5% dichloromethane, 5% acetonitrile and 5% water. Briefly, astaxanthin was extracted three times using a dichloromethane/methanol (1:1, v/v) solution. Then the extracts were collected and filtered for HPLC analysis (Higuera-Ciapara et al., 2004). The concentration of astaxanthin (μ g/ml) was calculated as the ratio between the amount of astaxanthin encapsulated in nanoparticles and the total volume of the ADC nanodispersion. The calibration of the peak area vs. astaxanthin concentration was linear in the range of the measured concentrations ($R^2 = 0.9975$, $n = 3$).

Residual ethanol in the prepared colloidal system was determined by headspace gas chromatography (HS-GC) according to the method of Zhang (Zhang, Lin, Chai, Zhong, & Barnes, 2015) with minor modifications. Methanol was used as the internal standard. The analysis was performed with an Agilent Technologies network GC system (7890 A, USA) interfaced to an Agilent 5975 C Mass Spectrometer, equipped with flame ionization detection, and controlled by a DB-1 fused silica capillary column of 30 m × 0.25 mm × 0.25 μ m (Supelco, Bellefonte, PA, USA). The measurements were operated at a temperature of 30 °C for 3 min with helium carrier gas. Each analysis was carried out in duplicate. Residual ethanol content (ppm) in sample *i* was calculated according to Eq. (1):

$$C_i = (A_i \times f_i \times C_{st}) / A_{st} \quad (1)$$

where C_i was the concentration of the component in sample, A_i was the chromatographic peak area of components in sample *i*, C_{st} was the concentration of internal standard, A_{st} was the chromatographic peak area of the internal standard and f_i was the component *i* correction factor.

2.4. Cytoprotective effect of ADC nanoparticles on H₂O₂-induced oxidative cell damage in Caco-2 cells

The ability of ADC nanoparticles to protect Caco-2 cells against H₂O₂-induced oxidative stress was examined. Different samples, including free astaxanthin (dissolved astaxanthin powder in 0.5% DMSO, 2 μ g/ml, i.e. 3.35 nM), ADC nanoparticles (with an astaxanthin concentration of 2 μ g/ml and a polymer concentration of 50 μ g/ml), DNA/chitosan (DNA/CS) nanocarriers (50 μ g/ml), and water-soluble vitamin C (2 μ g/ml, i.e. 10.58 nM) were used in this experiment. Caco-2 cells were seeded at a density of 1×10^5 /well in a black 96-well microplate in 100 μ l of cell culture medium per well. 24 h after seeding, the media were removed and the cells were respectively incubated with 100 μ l of the samples for another 24 h. Cells cultured with DMEM acted as control. Subsequently, the cells were treated with H₂O₂ solution (5.8 mM) for 1 h. The protective effect of ADC nanoparticles against oxidative damage to Caco-2 cells was expressed as relative cell viability rate. The cytotoxicity of the samples was simultaneously studied for comparison. To

assay for cell viability, 20 μ l/well MTT was added and incubated for 4 h. Then the supernatants were removed and 100 μ l of dimethyl sulfoxide (DMSO) was added. Plates were then placed in a shaking water bath at 37 °C for 10 min to dissolve the formazan salts, and subsequently the absorbance was measured at 570 nm. The protective effect of ADC nanoparticles against oxidative damage to Caco-2 cells was expressed as relative cell viability (RCV, %) by Eq. (2).

$$\text{RCV (\%)} = D_s/D_c \times 100\% \quad (2)$$

where D_s and D_c were the absorbance of the tested sample and the negative control, respectively.

2.5. ROS scavenging efficiency of ADC nanoparticles in Caco-2 cells

To further study the cell antioxidant effect of the antioxidants, free astaxanthin, ADC nanoparticles, DNA/CS nanocarriers and vitamin C (as mentioned in 2.4) were used for an ROS scavenging efficiency assay according to the method of Wolfe (Wolfe & Rui, 2007) with minor changes. Briefly, Caco-2 cells were grown in a 96-well microplate at a density of 1×10^5 /well and pretreated with the above samples for 24 h. The cells in culture media acted as negative control. Caco-2 cells in each well were washed twice with PBS and then incubated with 100 μ l of DCFH-DA (25 μ M) in antioxidant treatment medium for 1 h. Supernatants were then removed and the cells were washed once with 150 μ l of PBS. Finally, 100 μ l of H_2O_2 (5.8 mM) in medium was applied to each well. After 1 h, the fluorescent intensities were assayed using a fluorescence plate reader (λ_{ex} = 485 nm, λ_{em} = 535 nm). The general cellular antioxidant activity was expressed as ROS scavenging efficiency (RSE, %) by Eq. (3):

$$\text{RSE (\%)} = (1 - F_s/F_c) \times 100\% \quad (3)$$

where F_s and F_c were the fluorescence intensities of the tested sample well and the negative control, respectively.

2.6. Synthesis of FITC-labelled chitosan (FCS)

FITC-labelled chitosan (FCS) was synthesized based on the reaction between the amine groups of CS and the isothiocyanate group of FITC. Briefly, 40 mg of CS was dissolved in water (20 ml) in a weakly acidic condition with 0.1 M HCl, and the pH was adjusted to 6.9 with 0.05 M NaOH. FITC (4 mg) was firstly dissolved in 4 ml of methanol, and then added drop-wise in the CS solution. The mixture was stirred at room temperature for 6 h under light protection. After reaction, the solution was added in methanol/ammonium hydroxide (v/v = 7/3), then stirred by centrifuge (8000g) for 10 min to remove methanol. The precipitate was washed with 70% methanol to remove free FITC and freeze-dried to obtain the final product. The labelling efficiency for FCS was detected spectrometrically as Loh reported (Loh, Yeoh, Saunders, & Lim, 2010), and calculated as a percentage of FITC over the weight of FCS in the sample.

2.7. Preparation of FITC-labelled ADC (fADC) nanoparticles and cytotoxicity test

FITC-labelled ADC (fADC) nanoparticles were prepared as described in Section 2.2, except that FCS was used instead of CS. The cell viability was investigated by MTT assay (Li, Ma, Dang, Liang, & Chen, 2014). Briefly, Caco-2 and L929 cells were seeded at a density of 3×10^4 cells per well in 100 μ l of culture medium in 96-well culture plates and grown overnight. fADC nanodispersion was diluted in DMEM to a final polymer concentration ranging from 12.5 μ g/ml to 100 μ g/ml. 100 μ l of the above mentioned samples was added into each well. The cells in culture medium without

nanoparticles acted as control. After 48 h incubation, an MTT assay was performed as described in Section 2.4. The percentage viability was calculated using Eq. (2).

2.8. Cellular uptake of fADC nanoparticles

Caco-2 and L929 cells were seeded in a 96-well plate at a density of 3×10^4 cells per well for 24 h. Then the culture medium was replaced by phosphate-buffered saline (PBS, pH 7.4) and incubated at 37 °C for 0.5 h. After equilibration, the culture medium was exchanged for 100 μ l of freshly prepared fADC nanodispersion (25 μ g/ml) and incubated for 0.5 h, 1 h, and 4 h. At the predetermined time, the experiment was terminated by washing the cell monolayer three times with ice-cold phosphate-buffered saline. Each sample was observed using an inverted fluorescence microscope (Carl Zeiss, Germany). Afterwards, the cells were subjected to fluorescence quantitative analysis by adding 100 μ l of Triton X-100 (0.5%) to each well to lyse the cells (Hansen, Nielsen, & Berg, 1989). Cell-associated fADC nanoparticles were quantified by analyzing the cell lysate in a fluorescence plate reader (Bio-Tek Instruments, λ_{ex} = 485 nm, λ_{em} = 528 nm). The cellular uptake efficiency was calculated according to the following Eq. (4):

$$\text{Uptake efficiency (\%)} = W_s/W_T \times 100\% \quad (4)$$

where W_s and W_T were the amount of FITC in cell lysates and the total amount of FITC in the given FITC-labelled nanoparticles, respectively.

2.9. Statistical analyses

Unless otherwise indicated, all data are presented as mean \pm standard deviation (\pm SD). Statistical analysis was performed using one way ANOVA with $P < 0.05$ as significant. Calculations were done using the software SPSS 17.0.

3. Results and discussion

3.1. Preparation and characterization of ADC nanoparticles

To improve the water-dispensability and bioavailability of astaxanthin, natural DNA and chitosan were used in the current study to form nanocarriers for astaxanthin-encapsulation. ADC nanoparticles were prepared by the method of macromolecular co-assembly combined with solvent evaporation. Ethanol was used as a green organic solvent to dissolve astaxanthin, thus ensuring the biocompatibility and safety of the prepared nanosystem. ADC nanoparticles were prepared under the following conditions: the volume ratio of ethanol to water was 1:2; the molar ratio of the terminal amino groups in CS to the phosphate groups in DNA (N/P ratio) was 4:1. After removing ethanol by evaporation, a transparent and homogeneous astaxanthin-encapsulated colloidal system was successfully prepared and directly used for characterization.

The astaxanthin-encapsulated colloidal system with light red colour was stable with an obvious Tyndall effect (Fig. 1A). The morphology of the ADC nanoparticles was characterized by TEM and SEM. The TEM photo displays uniformly dispersed ADC nanoparticles with spherical shape (Fig. 1B), and the SEM photo also shows that the nanoparticles were well dispersed without any aggregation (Fig. 1C).

The zeta potential, average particle size and size distribution of ADC nanoparticles and DNA/CS nanocarriers were measured based on the Doppler micro-electrophoresis and the dynamic light scattering techniques. As expected, both ADC and DNA/CS nanoparticles prepared with an N/P ratio of 4:1 showed a positive surface charge,

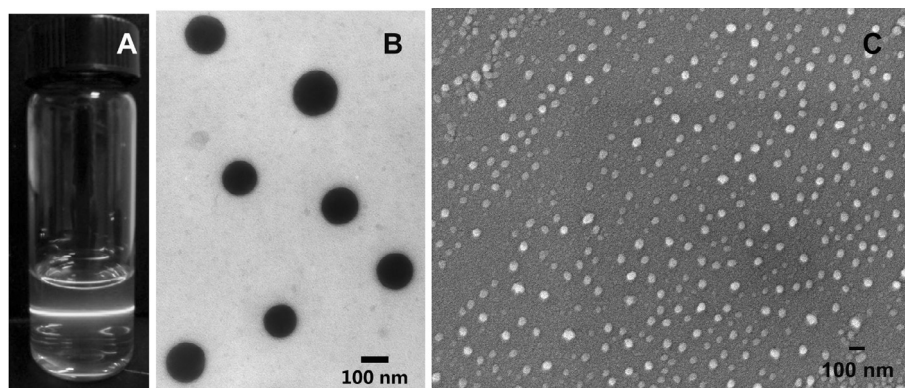


Fig. 1. The Tyndall effect (A) observed in ADC nanodispersion, TEM (B) and SEM (C) pictures of ADC nanoparticles.

Table 1
Particle size, size distribution and zeta potential of prepared nanoparticles.

Sample ID	Average size (nm)	PdI	Zeta potential (mV)
DNA/CS nanocarriers	92 ± 1	0.29 ± 0.01	32.2 ± 0.4
ADC	211 ± 5	0.29 ± 0.01	35.3 ± 1.1
fADC	237 ± 6	0.21 ± 0.01	29.3 ± 1.3

and the zeta potential of ADC and DNA/CS nanoparticles was 35.3 and 32.2 mV, respectively (Table 1). Their similar surface charge demonstrated that the embedded astaxanthin did not affect the zeta potential of the nanoparticles. The positive surface charge indicated that the predominant component, i.e. polycationic chitosan, was mainly distributed in the outer-shell of the nanoparticles. Notably, the average particle size of ADC nanoparticles was 211 ± 5 nm, with a polydispersity index (PdI) of 0.29 ± 0.01. This result demonstrated that the nanoparticles were uniform with proper size, which is consistent with the results of electron-microscopy observations. Moreover, the particle size of astaxanthin-loaded nanoparticles (ADC) was significantly larger than that of DNA/CS nanocarriers (92 nm, Table 1), which was mainly caused by the efficient entrapment of astaxanthin. As reported in the literature, the particle size of nanoparticles plays a significant role in adhesion and bio-interaction with cells, and the optimal size falls within the range of 100–300 nm (Couvreur & Puisieux, 1993). In this study, the ADC nanoparticles with a positive surface charge and a proper particle size are promising for cell uptake.

The concentration of astaxanthin in the prepared colloidal system determined by HPLC was 65 ± 4 µg/ml, which was higher than the solubility of astaxanthin in ethanol (approximately 35 µg/ml). Incidentally, the content of astaxanthin in dehydrated ADC nanoparticles reached as high as 40%, which was about 8-fold higher than that in *Haematococcus Pluvialis* (3–5%). This result suggests that DNA/CS nanoparticles make possible the encapsulation of large amounts of astaxanthin in the nano-scale delivery platform, and hence improve the water-dispersibility of astaxanthin. The efficient entrapment of astaxanthin in the nanocarriers is believed to directly react with DNA by intercalation or groove-binding, as well as enable entrapment into the hydrophobic micro-domains constructed by chitosan.

The residual amount of ethanol in the freshly prepared ADC nanodispersion measured by HS-GC was 890 ± 10 ppm. As a water-miscible solvent, it is difficult to completely remove ethanol from aqueous-based food systems due to the existence of azeotropic distillation points of the water-solvent mixture at which water tends to evaporate with this solvent below its boiling point

(Anarjan et al., 2012). The use of ethanol in food processing is acceptable only if its maximum daily intake is less than 5000 ppm (Witschi & Doelker, 1997). Therefore, the much lower solvent residual value (890 ppm) of the ADC nanodispersion herein confirmed its suitability for food and pharmaceutical application.

3.2. Cytoprotective effect of ADC nanoparticles against H₂O₂-induced oxidative cell damage in Caco-2 cells

The cytoprotective effect of ADC nanoparticles against H₂O₂-induced oxidative cell damage in Caco-2 cells was assessed by MTT assay. Treatment with 5.8 mM of H₂O₂ for 1 h produced 49.9% viable cells compared with 106.7% viable cells in control cultures (Fig. 2). ADC nanoparticles significantly prevented the deleterious effect of H₂O₂ on cell viability, and improved the cell viability from 49.9% to 61.9%. Compared with the group pre-treated with ADC nanoparticles, vitamin C (V_C) and free astaxanthin groups showed a lower cell viability rate of 59.9% and 51.3%, respectively, although the molarity of V_C was three times higher than astaxanthin. It should be mentioned that, the group pre-treated with DNA/CS nanocarriers showed similar cell viability (49.1%) to the group without pre-treatment, indicating that DNA/CS nanocarriers had little cytoprotective ability here. The results proved that ADC nanoparticles did obviously protect Caco-2 cells from oxidative damage, and had the strongest cytoprotective ability among the tested samples. Lu reported (Lu et al., 2010) that cell viability significantly increased from 63.9% to 73.9% when 500 nM of free astaxanthin was added to H₂O₂ treated neuronal cells. In the present study, only 3.35 nM of encapsulated astaxanthin in ADC nanodispersion showed an equivalent cytoprotective effect for H₂O₂ treated Caco-2 cells. Facilitated endocytosis of ADC nanoparticles was believed to be the main reason to display the antioxidant ability of the encapsulated-astaxanthin.

3.3. ROS scavenging efficiency of ADC nanoparticles in Caco-2 cells

To the best of our knowledge, astaxanthin is a powerful antioxidant that can scavenge the reactive oxygen species (ROS) *in vivo* and *in vitro* (Lee, Kim, & Yong, 2011), while few have reported the ROS generation-suppressing effect of astaxanthin-loaded colloidal system at a cellular level. As a novel astaxanthin-loaded colloidal system, ADC nanoparticles were used to scavenge the ROS in H₂O₂-treated Caco-2 cells. As shown in Fig. 3, the ROS scavenging efficiency of ADC nanoparticles was 54.3%, which was 2-fold higher than that of free astaxanthin (26.8%) in the case of the same astaxanthin concentration (3.35 nM). As a positive control, V_C that scavenges ROS directly (Gotoh & Niki, 1992), showed similar ROS scavenging efficiency (27.3%) to free astaxanthin, even though

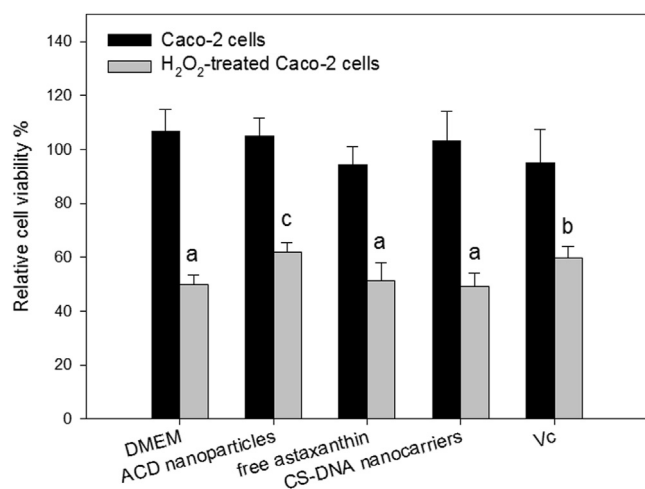


Fig. 2. The cell viability of Caco-2 cells and H₂O₂-treated Caco-2 cells in the different treatment groups (n = 6). ^{a-c}Different letters show statistically significant differences (*P* < 0.05) between similar responses.

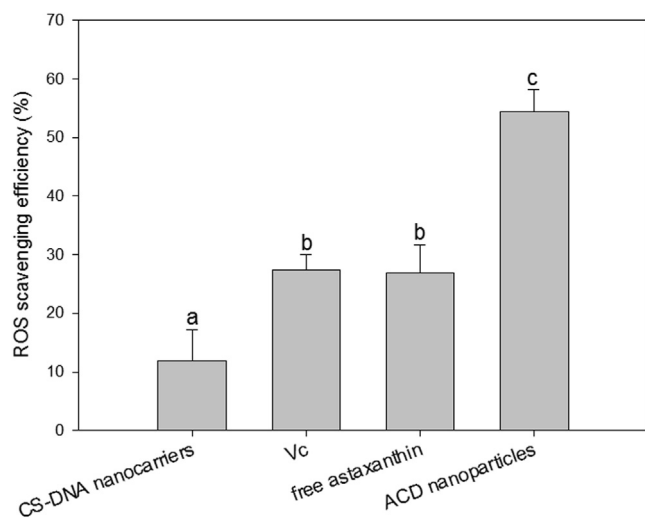


Fig. 3. The ROS scavenging efficiency of different samples (DNA/CS nanocarriers, Vc, free astaxanthin and ADC nanoparticles) in Caco-2 cells (n = 4). ^{a-c}Different letters show statistically significant differences between values of ROS scavenging efficiency (*P* < 0.05).

the molarity of Vc (10.58 nM) was 3-fold higher than astaxanthin (3.35 nM). As was reported, astaxanthin with a concentration of more than 100 nM has the ability to suppress ROS generation in the cells (Liu & Osawa, 2007), and prevents UVA-induced DNA damage in 1BR-3 cells at a minimal concentration of 10 nM (Lyons & O'Brien, 2002). In this study, ADC nanodispersion with a final astaxanthin concentration of 3.35 nM in the reaction system already significantly suppressed ROS generation in H₂O₂-treated Caco-2 cells. The result might be attributed to three accounts as follows. Firstly, the positive surface charge of the DNA/CS nanocarriers (32.2 mV, see in Table 1) facilitated the cellular uptake of the astaxanthin-loaded nanoparticles, which enabled the encapsulated-astaxanthin to gradually accumulate to a higher level in cells and provided improved ROS scavenging efficiency. Secondly, by loading in the nanocarriers, the stability of the encapsulated astaxanthin improved, making it effectively quench the intracellular free radicals and reactive oxygen species. Thirdly, the DNA/CS nanocarriers themselves also showed a certain ROS scavenging ability (11.9%) due to the presence of DNA that could

be oxidatively damaged by exogenous H₂O₂ (Santocono, Zurria, Berrettini, Fedeli, & Falcioni, 2006). Therefore, it can be stated that the prepared ADC colloidal system showed better antioxidant activity than free astaxanthin at a cellular level, which is consistent with the results in Section 3.2.

3.4. Preparation and cytotoxicity test of FITC-labelled ADC (fADC) nanoparticles

In this study, fluorescent nanoparticles were prepared using CS tagged with FITC for tracing nanoparticles *in vitro*. The labelling efficiency of FITC-labelled chitosan (FCS) was 1%. Astaxanthin-loaded nanoparticles prepared using the FCS, i.e. fADC, nanoparticles were comparable to ADC nanoparticles in that they had an average particle size of 237 nm (Table 1). Prior to evaluation of cellular uptake of fADC nanoparticles, the cytotoxicity was tested and the concentration of added nanoparticles for *in vitro* experiments was optimized. L929 and Caco-2 cells were employed as normal and tumor cell models. As shown in Fig. 4, the Caco-2 and L929 cells retained more than 90% viability when treated with fADC nanoparticles for 48 h to a maximum concentration of 100 µg/ml. In particular, Caco-2 cells treated with fADC nanoparticles of less than 25 µg/ml showed relatively high cell viabilities (>110%), indicating that even a small amount of fADC nanoparticles can play a considerable growth promoting effect on cells due to the bioactivity of astaxanthin. Therefore, fADC nanodispersion with a polymer concentration of 25 µg/ml was used for the follow-up cellular uptake study. Generally speaking, fADC nanoparticles showed no cytotoxicity to either normal or tumor cells when the concentration was below 100 µg/ml, as stated in the third edition of International Standard (ISO 10993-5, Tests for *in vitro* cytotoxicity).

3.5. Cellular uptake of fADC nanoparticles

Cellular uptake of fADC nanoparticles was studied to analyze the absorption mechanism of astaxanthin by fibroblasts and epithelial cells via an endocytosis pathway. FITC-labelled nanoparticles facilitated cell observation and quantitative detection. Caco-2 intestinal epithelia cells that secrete extracellular mucus and large lipoproteins were selected as an epithelial cell model, while L929 fibroblasts that synthesize the extracellular matrix and collagen were used as a fibroblast cell model. Cellular uptake of fADC nanoparticles after co-incubating for 0.5 h, 1 h, and 4 h was confirmed via fluorescence microscopy (Fig. 5A). A tendency of increasing fluorescent intensity during 4 h co-incubation was observed in both cells. Notably, after 0.5 h of co-incubation, the fluorescence intensity in Caco-2 cells was significantly higher than in L929 cells. The results demonstrated that: (1) cellular uptake of fADC nanoparticles did happen in both cell lines, which further proves the findings in Sections in 3.1 and 3.2. (2) Compared to L929 cells, Caco-2 cells showed quicker uptake of fADC nanoparticles due to their different extracellular environments. (3) The positive surface charge of the nanoparticles (29.3 mV, see in Table 1) enhanced the permeability of the cell membrane to fADC nanoparticles, which resulted in increased cellular uptake during 4 h incubation (Mao et al., 2004; K.K. Yang et al., 2013).

Meanwhile, the uptake efficiency of fADC nanoparticles in Caco-2 and L929 cells with certain incubation times were quantitatively analyzed by fluorescence spectrophotometry. The uptake rates of fADC nanoparticles increased from 0.13% to 0.26% during 4 h co-incubation in Caco-2 cells, while the uptake rates increased from 0.07% to 0.15% in L929 cells (Fig. 5B). This result verified expectations that the endocytosis of fADC nanoparticles was a fast process: the cellular uptake rate of fADC nanoparticles abruptly increased in one hour, followed by a slow increase within 4 h. It was also found that the uptake efficiency in Caco-2 cells was about

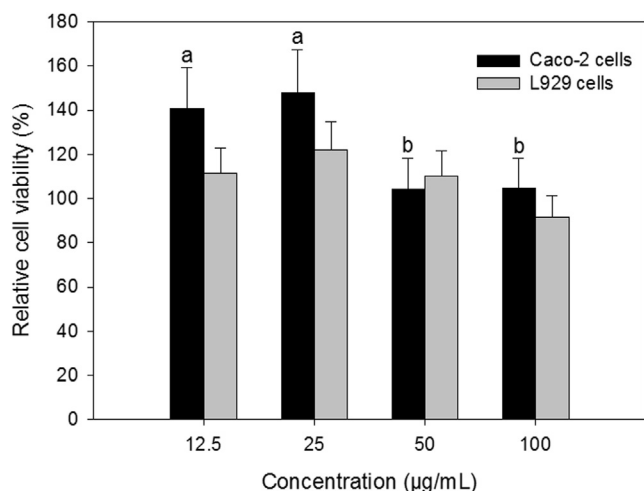


Fig. 4. *In vitro* cytotoxicity of fADC nanoparticles in Caco-2 and L929 cells for 48 h. ^{a,b}Different letters show statistically significant differences between values of cell viability ($P < 0.05$).

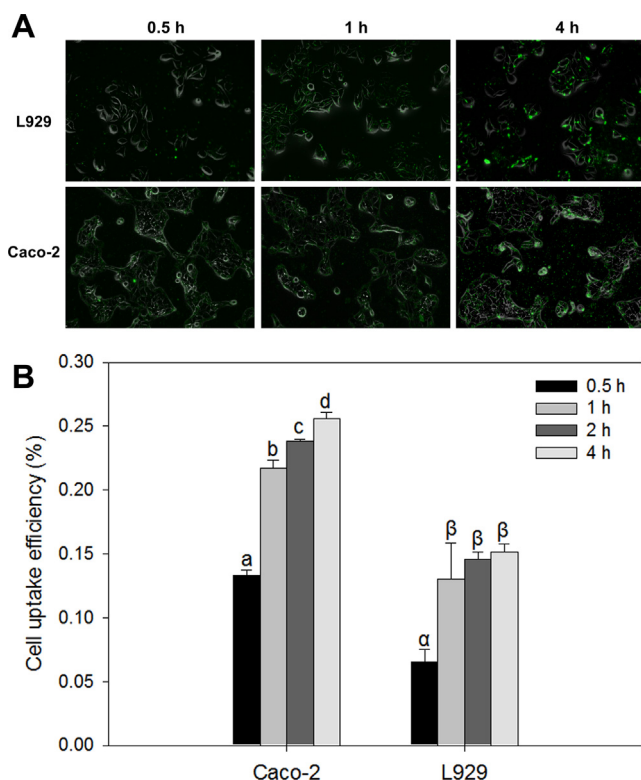


Fig. 5. A: Microscope images of L929 and Caco-2 cells incubated with fADC nanoparticles (25 µg/mL) at 37 °C for 0.5, 1 and 4 h (fluorescence and transmitted light images merged). B: The cellular uptake efficiency of fADC nanoparticles in Caco-2 and L929 cells with certain incubation times. ^{a-d,α,β}Different letters show statistically significant differences ($P < 0.05$) between experimental response values in which the comparison tests were performed between similar responses.

2-fold higher than that of L929 cells. As is well known, the extracellular mucus and large lipoproteins that Caco-2 cells secrete plays a supporting role for the capture of nanoparticles as well as for the absorption of fat-soluble nutrients, such as carotenoids (During, Hussain, Morel, & Harrison, 2002), while the extracellular matrix and collagen that L929 cells secretes hinders the interaction between nanoparticles and cells. The facilitated cellular uptake of fADC nanoparticles by intestinal epithelial cells indicates that

endocytosis is an effective way for astaxanthin absorption *in vivo*. It should be noted that the decelerated cellular uptake of fADC nanoparticles was mainly caused by the negatively charged groups in the cell culture medium that collaboratively weakened the surface charge of the nanoparticles and hence weakened the adhesion of nanoparticles to the negatively charged cell membrane.

4. Conclusions

In conclusion, astaxanthin-loaded DNA/CS (ADC) nanoparticles with spherical shape and uniform size were successfully prepared. The obtained homogeneous and transparent ADC nanodispersion with astaxanthin content up to 65 µg/mL, not only ensured the water-solubility and stability of astaxanthin, but also enhanced its cellular uptake efficiency. According to the present study, FITC-labelled ADC nanoparticles were easily engulfed by Caco-2 cells due to its extracellular matrix, which indicated that the astaxanthin in ADC nanoparticles could be absorbed through an endocytic pathway. By entrapping liposoluble astaxanthin in hydrophilic nanocarriers, ADC nanoparticles showed more powerful antioxidant activity than free astaxanthin, by improving the cytoprotective effect and ROS scavenging efficiency on H_2O_2 -induced oxidative cell damage in Caco-2 cells. This novel astaxanthin-loaded colloidal system with improved cellular uptake and antioxidant capability has the potential to be widely used in the fields of functional food, cosmetics and medicine.

Acknowledgements

This work was supported by the National Natural Science Foundation of China [grant numbers 31301420, 31571937]; a China Postdoctoral Science Foundation funded project [grant number 2014M551965]; and the NSFC-Shandong Joint Fund for Marine Science Research Centers [grant number U1406402].

References

- Anarjan, N., Tan, C. P., Nehdi, I. A., & Ling, T. C. (2012). Colloidal astaxanthin: preparation, characterisation and bioavailability evaluation. *Food Chemistry*, 135(3), 1303–1309.
- Behrens, I., Pena, A. I. V., Alonso, M. J., & Kissel, T. (2002). Comparative uptake studies of bioadhesive and non-Bioadhesive nanoparticles in human intestinal cell lines and rats: The effect of mucus on particle adsorption and transport. *Pharmaceutical Research*, 19(8), 1185–1193.
- Bustos-Garza, C., Yáñez-Fernández, J., & Barragán-Huerta, B. E. (2013). Thermal and pH stability of spray-dried encapsulated astaxanthin oleoresin from *Haematococcus pluvialis* using several encapsulation wall materials. *Food Research International*, 54(1), 641–649.
- Couvreur, P., & Puisieux, F. (1993). Nano- and microparticles for the delivery of polypeptides and proteins. *Advanced Drug Delivery Reviews*, 10(2), 141–162.
- Cui, Z., & Mumper, R. J. (2001). Chitosan-based nanoparticles for topical genetic immunization. *Journal of Controlled Release*, 75(3), 409–419.
- During, A., Hussain, M. M., Morel, D. W., & Harrison, E. H. (2002). Carotenoid uptake and secretion by Caco-2 cells: Beta-carotene isomer selectivity and carotenoid interactions. *Journal of Lipid Research*, 43(7), 1086–1095.
- Gotoh, N., & Niki, E. (1992). Rates of interactions of superoxide with vitamin E, vitamin C and related compounds as measured by chemiluminescence. *Biochimica Et Biophysica Acta*, 1115(3), 201–207.
- Hansen, J. C. (2002). Conformational dynamics of the chromatin fiber in solution: Determinants, mechanisms, and functions. *Annual Review of Biophysics and Biomolecular Structure*, 31, 361–392.
- Hansen, M. B., Nielsen, S. E., & Berg, K. (1989). Re-examination and further development of a precise and rapid dye method for measuring cell growth/cell kill. *Journal of Immunological Methods*, 119(2), 203–210.
- Higuera-Ciarpaga, I., Felix-Valenzuela, L., Goycoolea, F., & Argüelles-Monal, W. (2004). Microencapsulation of astaxanthin in a chitosan matrix. *Carbohydrate Polymers*, 56(1), 41–45.
- Kittikawan, P., Powthongsook, S., Pavasant, P., & Shotipruk, A. (2007). Encapsulation of *Haematococcus pluvialis* using chitosan for astaxanthin stability enhancement. *Carbohydrate Polymers*, 70(4), 378–385.
- Kulkarni, S. A., & Feng, S. S. (2013). Effects of particle size and surface modification on cellular uptake and biodistribution of polymeric nanoparticles for drug delivery. *Pharmaceutical Research*, 30(10), 2512–2522.

- Layek, B., & Singh, J. (2017). 8-Chitosan for DNA and gene therapy. In J. A. Jennings & J. D. Burngardner (Eds.), *Chitosan based biomaterials (Volume 2): Tissue Engineering and Therapeutics* (pp. 209–244). Woodhead publishing.
- Lee, D. H., Kim, C. S., & Yong, J. L. (2011). Astaxanthin protects against MPTP/MPP+-induced mitochondrial dysfunction and ROS production in vivo and in vitro. *Food and Chemical Toxicology*, 49(1), 271–280.
- Li, L., Li, J., Si, S., Wang, L., Shi, C., Sun, Y., ... Mao, S. (2015). Effect of formulation variables on in vitro release of a water-soluble drug from chitosanesodium alginate matrix tablets. *Asian Journal of Pharmaceutical Sciences*, 10(4), 314–321.
- Li, J., Ma, F. K., Dang, Q. F., Liang, X. G., & Chen, X. G. (2014). Glucose-conjugated chitosan nanoparticles for targeted drug delivery and their specific interaction with tumor cells. *Frontiers of Materials Science*, 8(4), 363–372.
- Liu, X., & Osawa, T. (2007). Cis astaxanthin and especially 9-cis astaxanthin exhibits a higher antioxidant activity in vitro compared to the all-trans isomer. *Biochemical and Biophysical Research Communications*, 357(1), 187–193.
- Loh, J. W., Yeoh, G., Saunders, M., & Lim, L. Y. (2010). Uptake and cytotoxicity of chitosan nanoparticles in human liver cells. *Toxicology and Applied Pharmacology*, 249(2), 148–157.
- Lu, Y. P., Liu, S. Y., Sun, H., Wu, X. M., Li, J. J., & Zhu, L. (2010). Neuroprotective effect of astaxanthin on H₂O₂-induced neurotoxicity in vitro and on focal cerebral ischemia in vivo. *Brain Research*, 1360, 40–48.
- Lyons, N. M., & O'Brien, N. M. (2002). Modulatory effects of an algal extract containing astaxanthin on UVA-irradiated cells in culture. *Journal of Dermatological Science*, 30(1), 73–84.
- Majeed, A. (2011). Development and stability evaluation of astaxanthin nanoemulsion. *Asian Journal of Pharmaceutical and Clinical Research*, 4(1), 142–148.
- Mao, C., Zhu, J. J., Hu, Y. F., Ma, Q. Q., Qiu, Y. Z., Zhu, A. P., ... Shen, J. (2004). Surface modification using photocrosslinkable chitosan for improving hemocompatibility. *Colloids and Surfaces B: Biointerfaces*, 38(1–2), 47–53.
- Mohammadi, Z., Dorkoosh, F. A., Hosseinkhani, S., Gilani, K., Amini, T., Najafabadi, A. R., & Tehrani, M. R. (2011). In vivo transfection study of chitosan-DNA-FAP-B nanoparticles as a new non viral vector for gene delivery to the lung. *International Journal of Pharmaceutics*, 421(1), 183–188.
- Naguib, Y. M. A. (2000). Antioxidant activities of astaxanthin and related carotenoids. *Journal of Agricultural and Food Chemistry*, 48(4), 1150–1154.
- Park, S. A., Ahn, J. B., Choi, S. H., Lee, J. S., & Lee, H. G. (2014). The effects of particle size on the physicochemical properties of optimized astaxanthin-rich *Xanthophyllomyces dendrorhous*-loaded microparticles. *LWT-Food Science and Technology*, 55(2), 638–644.
- Peng, C. H., Chang, C. H., Peng, R. Y., & Chyau, C. C. (2010). Improved membrane transport of astaxanthine by liposomal encapsulation. *European Journal of Pharmaceutics and Biopharmaceutics*, 75(2), 154–161.
- Santocono, M., Zurria, M., Berrettini, M., Fedeli, D., & Falcioni, G. (2006). Influence of astaxanthin, zeaxanthin and lutein on DNA damage and repair in UVA-irradiated cells. *Journal of Photochemistry and Photobiology B: Biology*, 85(3), 205–215.
- Sonaje, K., Lin, Y. H., Juang, J. H., Wey, S. P., Chen, C. T., & Sung, H. W. (2009). In vivo evaluation of safety and efficacy of self-assembled nanoparticles for oral insulin delivery. *Biomaterials*, 30(12), 2329–2339.
- Tachaprutinun, A., Udomsup, T., Luadthong, C., & Wanichwecharungruang, S. (2009). Preventing the thermal degradation of astaxanthin through nanoencapsulation. *International Journal of Pharmaceutics*, 374(1–2), 119–124.
- Thanou, M., Verhoef, J. C., & Junginger, H. E. (2001). Oral drug absorption enhancement by chitosan and its derivatives. *Advanced Drug Delivery Reviews*, 52(52), 117–126.
- Witschi, C., & Doelker, E. (1997). Residual solvents in pharmaceutical products: acceptable limits, influences on physicochemical properties, analytical methods and documented values. *European Journal of Pharmaceutics and Biopharmaceutics*, 43(3), 215–242.
- Wolfe, K. L., & Rui, H. L. (2007). Cellular antioxidant activity (CAA) assay for assessing antioxidants, foods, and dietary supplements. *Journal of Agricultural and Food Chemistry*, 55(22), 8896–8907.
- Yamamoto, H., Kuno, Y., Sugimoto, S., Takeuchi, H., & Kawashima, Y. (2005). Surface-modified PLGA nanosphere with chitosan improved pulmonary delivery of calcitonin by mucoadhesion and opening of the intercellular tight junctions. *Journal of Controlled Release*, 102(2), 373–381.
- Yan, J., Du, Y. Z., Chen, F. Y., You, J., Yuan, H., & Hu, F. Q. (2013). Effect of proteins with different isoelectric points on the gene transfection efficiency mediated by stearic acid grafted chitosan oligosaccharide micelles. *Molecular Pharmaceutics*, 10(7), 2568–2577.
- Yang, K., Gao, T., Bao, Z., Su, J., & Chen, X. (2013). Preparation and characterization of a novel thermosensitive nanoparticle for drug delivery in combined hyperthermia and chemotherapy. *Journal of Materials Chemistry B*, 1(46), 6442–6448.
- Yang, K. K., Kong, M., Wei, Y. N., Liu, Y., Cheng, X. J., Li, J., ... Chen, X. G. (2013). Folate-modified-chitosan-coated liposomes for tumor-targeted drug delivery. *Journal of Materials Science*, 48(4), 1717–1728.
- Yue, Y., Jin, F., Deng, R., Cai, J., Chen, Y., Lin, M. C., ... Wu, C. (2011). Revisit complexation between DNA and polyethylenimine – Effect of uncomplexed chains free in the solution mixture on gene transfection. *Journal of Controlled Release*, 155(1), 67–76.
- Zhang, C. Y., Lin, N. B., Chai, X. S., Zhong, L., & Barnes, D. G. (2015). A rapid method for simultaneously determining ethanol and methanol content in wines by full evaporation headspace gas chromatography. *Food Chemistry*, 183, 169–172.
- Zhao, Q. S., Ji, Q. X., Cheng, X. J., Sun, G. Z., Ran, C., Zhao, B., & Chen, X. G. (2010). Preparation of alginate coated chitosan hydrogel beads by thermosensitive internal gelation technique. *Journal of Sol–Gel Science and Technology*, 54(2), 232–237.